

Review

Review on the Application of Supplementary Cementitious Materials in Self-Compacting Concrete

Lang Pang ¹, Zhenguo Liu ², Dengquan Wang ^{3,*} and Mingzhe An ¹

¹ School of Civil Engineering, Beijing Jiaotong University, Beijing 100044, China; 20121088@bjtu.edu.cn (L.P.); mzhan@bjtu.edu.cn (M.A.)

² Beijing Urban Construction Group, Beijing 100023, China; liuzhenguothu@163.com

³ Department of Civil Engineering, Tsinghua University, Beijing 100084, China

* Correspondence: wangdq16@mails.tsinghua.edu.cn; Tel.: +86-188-1135-1597

Abstract: For the sustainable development of construction materials, supplementary cementitious materials (SCMs) are commonly added to self-compacting concrete (SCC). This paper reviewed the application techniques and hydration mechanisms of SCMs in SCC. The impacts of SCMs on the microstructure and performance of SCC were also discussed. SCMs are used as a powder material to produce SCC by replacing 10% to 50% of cement. Hydration mechanisms include the pozzolanic reaction, alkaline activation, and adsorption effect. Moreover, the filling effect and dilution effect of some SCMs can refine the pore structure and decrease the temperature rise of concrete, respectively. Specifically, the spherical particles of fly ash can improve the fluidity of SCC, and the aluminum-containing mineral phase can enhance the resistance to chloride ion penetration. Silica fume will increase the water demand of the paste and promote its strength development (a replacement of 10% results in a 20% increase at 28 days). Ground-granulated blast furnace slag may reduce the early strength of SCC. The adsorption of Ca^{2+} by CaCO_3 in limestone powder can accelerate the hydration of cement and promote its strength development.

Keywords: self-compacting concrete; supplementary cementitious materials; hydration mechanisms; microstructure; fresh properties



Citation: Pang, L.; Liu, Z.; Wang, D.; An, M. Review on the Application of Supplementary Cementitious Materials in Self-Compacting Concrete. *Crystals* **2022**, *12*, 180. <https://doi.org/10.3390/cryst12020180>

Academic Editors: Yifeng Ling, Chuanqing Fu, Peng Zhang, Peter Taylor and Helmut Cölfen

Received: 1 December 2021

Accepted: 24 January 2022

Published: 26 January 2022

Publisher's Note: MDPI stays neutral with regard to jurisdictional claims in published maps and institutional affiliations.



Copyright: © 2022 by the authors. Licensee MDPI, Basel, Switzerland. This article is an open access article distributed under the terms and conditions of the Creative Commons Attribution (CC BY) license (<https://creativecommons.org/licenses/by/4.0/>).

1. Introduction

Self-compacting concrete (SCC) is a type of high-performance concrete that can be poured into structural formwork by gravity and compacted without vibration. Okamura et al. [1] pioneered the application of SCC in Japan in 1988. The outstanding features are that SCC eliminates the mechanical vibration process and lowers labor costs as compared to normal vibrating concrete (NVC), and SCC has a high powder material content in the mixture to increase fresh properties (Figure 1). However, using cement solely as a powder material leads to high production cost for SCC, which restricts its wide use. In addition, the high cement content in SCC poses increasing environmental risks as cement production is a high-resource-consuming and waste-discharging process, and its annual production has reached 3000 million tons worldwide [2].

SCC	A	W	Powder	S	G
Air		Water	SCMs can be added	Fine aggregate	Coarse aggregate
NVC	A	W	Cement	S	G

Figure 1. Comparison of component proportions between SCC and NVC [1].

The addition of supplementary cementitious materials (SCMs) as a partial substitute for cement can significantly lower the production cost of SCC as well as relieve the shortages of cement raw materials and solid waste pollution [3]. SCMs can adjust the fresh properties and improve the durability properties [4]. Specifically, SCMs can effectively enhance the microstructure of SCC. Furthermore, SCMs will have superposition effects when two or more of them are used together. Although SCMs have been widely employed in SCC, there is still a lack of a summary in its mix proportions. Moreover, the functions of SCMs in SCC remain unclear, and the systematic analysis of macroscopic properties does not exist yet. Therefore, it is necessary to outline the influences of SCMs in SCC, which can promote the sustainable development of SCC technology and improve the comprehensive utilization of solid wastes. The application techniques and hydration mechanisms of SCMs in SCC were reviewed in this work, and the impacts of fly ash (FA), silica fume (SF), ground granulated blast furnace slag (GBFS), and limestone powder (LP) on the microstructure and performance of SCC were also summarized.

2. Mixture Design of SCC

The fresh paste of SCC should have high fluidity as well as resistance to segregation and bleeding during pouring, especially when the paste flows through the limited space of reinforcing bars. It should be noted that the higher the proportion of coarse aggregate in concrete, the smaller the relative distance between particles, which increases the frequency of collision and friction. As a result, the internal stress caused by coarse aggregate consumes a large amount of energy for flowing, which reduces the fresh properties of the paste and even causes blockage. To avoid this, Okamura et al. [1] initially modified the mix proportion by reducing aggregate content, increasing powder content, and adding superplasticizer. To generate self-compacting concrete, this work first sets the amount of aggregate and next changes the water-to-binder ratio and superplasticizer dosages. Figure 1 depicts the proportion of each component. In China, the mixture proportion design of SCC is often done by the absolute volume technique (Chinese standard: CECS203, 2006). In this technique, the cement paste that meets the performance requirements is prepared first, and the fine and coarse aggregates are added sequentially to produce the appropriate mortar and concrete. In addition, Wu et al. [5] and Nie et al. [6] have proposed a mix design method based on the rheological characteristics of paste.

It can be found that SCC contains a larger proportion of powder material than NVC. Domone [7] summarized a lot of instances from previous research and discovered that roughly 95% of self-compacting concrete had powder masses of more than 400 kg/m³. This demonstrates that more SCMs can be added to SCC. The application of SCMs reduces the production costs of SCC while improving concrete performance. For example, adding FA can improve the fresh properties of SCC [8], and adding SF can enhance its strength properties [9]. Moreover, the viscosity modifying admixture should be added to stabilize the rheology and setting time when segregation occurs due to the addition of high-content or composite SCMs [10].

3. Material Characteristics

3.1. Characteristics of SCMs

The most common SCMs used in SCC are fly ash, silica fume, ground granulated blast furnace slag, and limestone powder. In addition, some other SCMs with fewer use cases are also used in SCC, such as copper slag [11], zeolite powder [12], etc. From the results of existing studies, the percentages of SiO₂, Al₂O₃, and CaO in FA, SF, GBFS, LP, and cement were compared and shown in Figure 2. FA has the highest Al₂O₃ content; GBFS mainly contains SiO₂ and CaO; the chemical composition of SF and LP is relatively simple, containing only SiO₂ and CaCO₃, respectively. It is worth noting that the chemical composition of the same kind of SCM varies greatly due to the considerable variances in the raw ore, manufacturing procedure, and discharge process. Compared with SCMs, Portland

cement is more concentrated in the areas shown in Figure 2, and its chemical composition is more stable.

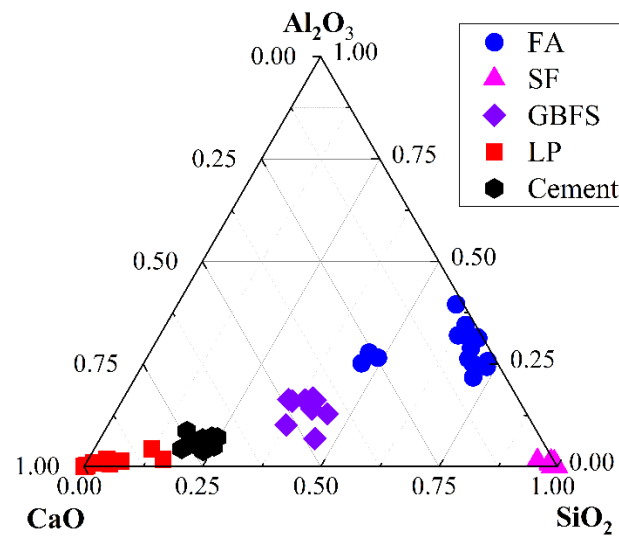


Figure 2. Chemical composition of FA [8,13–25], SF [9,26–41], GBFS [42–54], LP [55–63], and cement [19–28,38–40,64–66].

The microscopic images of FA, SF, GBFS, and LP are shown in Figure 3. It can be found that the FA is mostly smooth and spherical particles, and this spherical shape can play a ball-bearing role in the freshly mixed SCC. The particle sizes of SF are usually small, and it will typically increase the water demand of fresh paste. GBFS and LP show obvious irregular and angular shapes due to mechanical grinding.

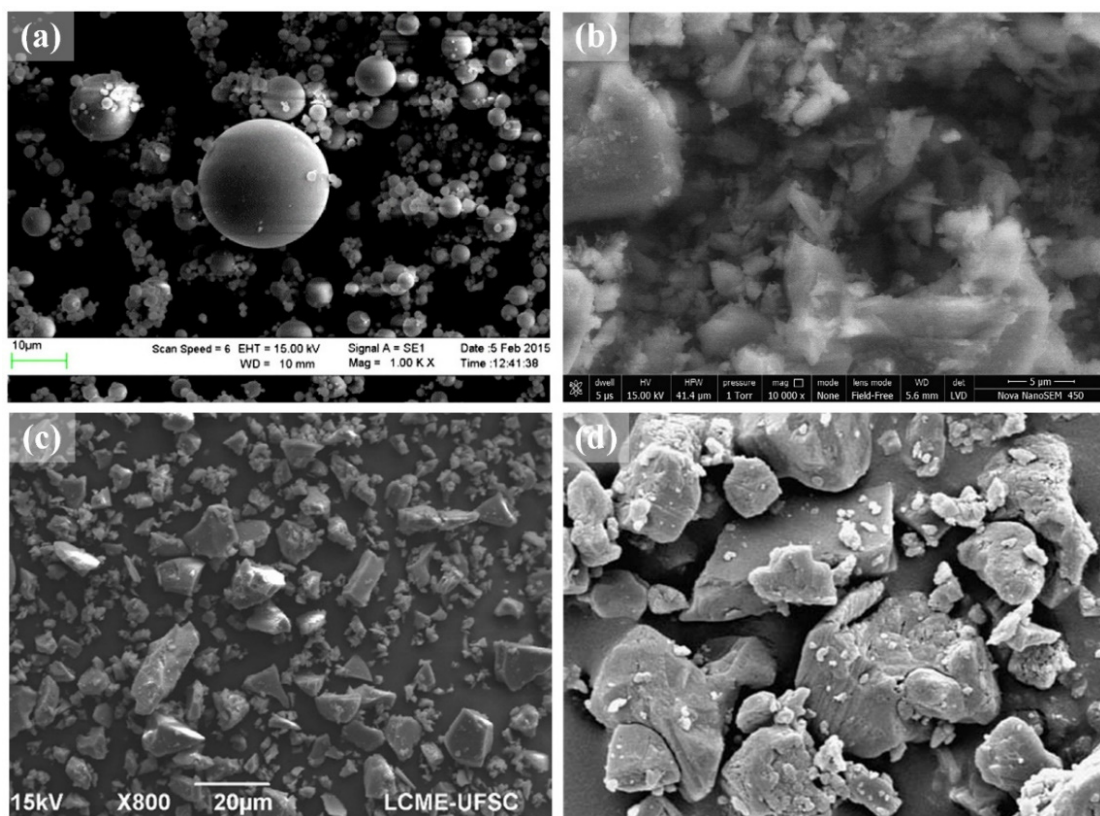
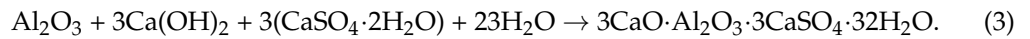
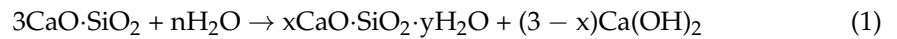


Figure 3. Microscopic image of SCMs: (a) FA [23], (b) SF [17], (c) GBFS [50], (d) LP [67].

3.2. Hydration Mechanisms

The hydration processes of Portland cement can be divided into three periods: the induction period, the acceleration period, and the deceleration period [68]. When SCMs are incorporated into SCC, the hydration process of the composite system is significantly influenced by SCMs (Figure 5). The hydration process in the composite system usually involves the cement first hydrating to produce primary hydration products; then, the products react with SCMs to produce secondary hydration products. For example, the hydration of GBFS is triggered by the deconstruction of the glass by OH⁻ generated from the hydration of cement, which serves as an alkaline activator. This process releases the ions in the glass (Ca²⁺, Al³⁺, SiO₄⁴⁻, etc.) into the solution for subsequent hydration. The main reaction product of GBFS by alkaline activation is a type of aluminum-substituted C-A-S-H gel, which presents a disordered tobermorite-like C-S-H type structure. In addition, the active Al₂O₃ in GBFS will further react with Ca(OH)₂ and gypsum (CaSO₄) to form ettringite (AFt) [69,70]. These reactions are shown in Equations (1)–(3) as follows:



For the C-A-S-H gel, existing studies have shown that when the paste contains Na⁺, the chemically bound Ca²⁺ in C-A-S-H will be replaced by Na⁺ to form a C(N)-A-S-H type gel [71]. Myers et al. [72] proposed a structural model to simulate this gel based on the cross-linked and non-cross-linked structure properties of C(N)-A-S-H, as shown in Figure 4.

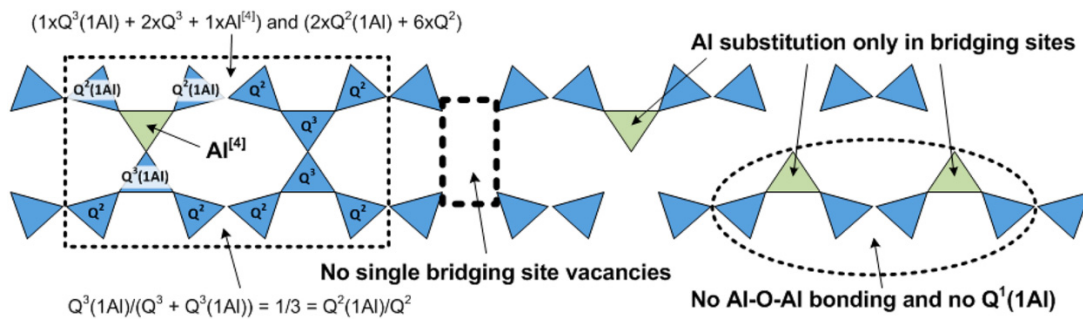


Figure 4. The cross-linked and non-cross-linked structures of the C(N)-A-S-H type gel [72].

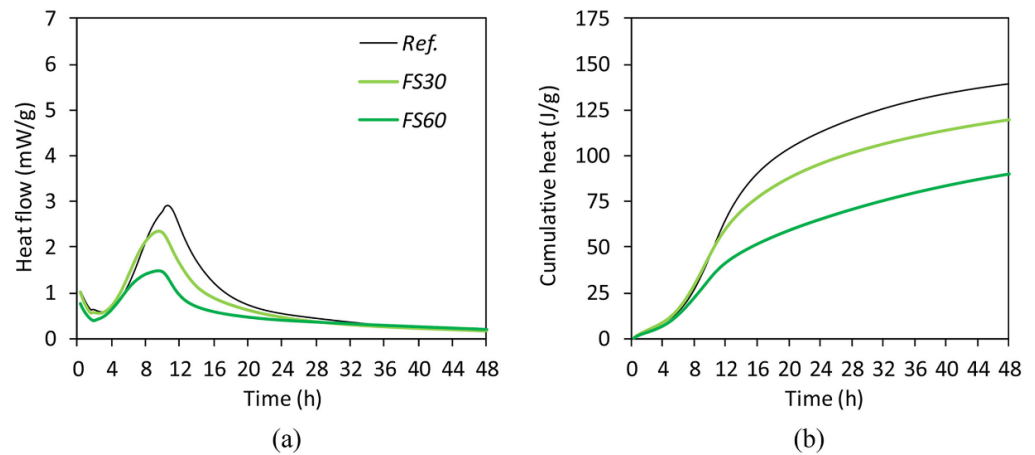


Figure 5. Isothermal calorimetry curves for the paste mixed with GGBS: (a) heat flow and (b) cumulative heat [73].

Similar to the hydration process of GBFS, the hydration of FA occurs under the alkali activity of OH^- produced by cement hydration. However, FA is less active due to its high amount of SiO_2 and Al_2O_3 (low $\text{Ca}/(\text{Si} + \text{Al})$ ratio) and stable Si-O and Al-O bonds. Its contribution to hydration is generally apparent at a later stage. Fernandez et al. [74] developed a microstructural model for the hydration process of FA, as illustrated in Figure 6. The attack on the incomplete spherical glassy shell of FA particles by OH^- causes the formation of reaction products both inside and outside, and finally, FA particles with various reaction degrees will be embedded in the microstructure. It is worth pointing out that SCMs can offer nucleation sites for cement hydration in addition to the secondary reaction with the primary products. For instance, the chemical adsorption of Ca^{2+} by the surface of limestone particles can effectively enhance the nucleation and growth of C-S-H; silica fume can adsorb Ca^{2+} via electrostatic force and boost the formation of hydration products [75].

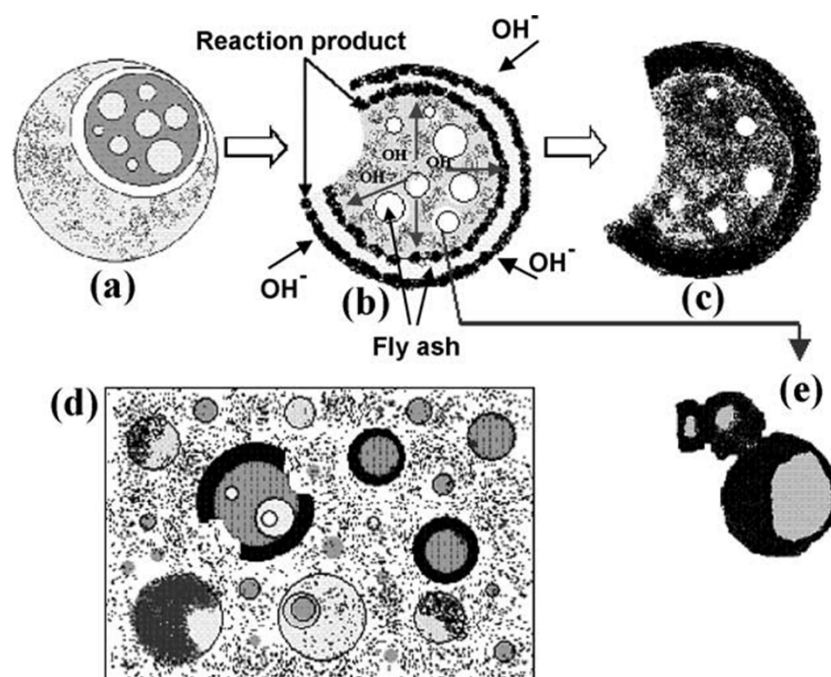


Figure 6. Descriptive model of the reaction process of fly ash: (a) initial chemical attack, (b) bi-directional alkaline attack, (c) reaction product, (d) several morphologies and (e) products covers certain portions [74].

4. Influence of SCMs in SCC

4.1. Microstructure

Concrete consists of three parts: aggregate, interfacial transition zone (ITZ), and cement paste. ITZ is a thin shell wrapped around the surface of the aggregate and is the lowest-strength part of concrete, whose microstructure determines the performance of concrete [76]. The incorporated SCMs can influence the formation and development of the ITZ in SCC. Figure 7 shows the comparison of the ITZ between SCC without SCMs and mixed with 20% and 30% fly ash [25]. The influences originate from three effects of SCMs: namely, the filling effect, pozzolanic reaction, and dilution effect. The filling effect can increase the packing density and optimize the mixture proportion of concrete. At the same time, the pozzolanic reaction of SCM can consume the CH generated by cement hydration while creating C-S-H, thus improving the interfacial transition zone. In addition, the fact of a general slower hydration reaction of SCM allows for more water to participate in cement hydration, resulting in an adequate reaction of cement. Simultaneously, SCMs can offer nucleation sites for cement hydration, resulting in more evenly dispersed reaction products (Figure 8).

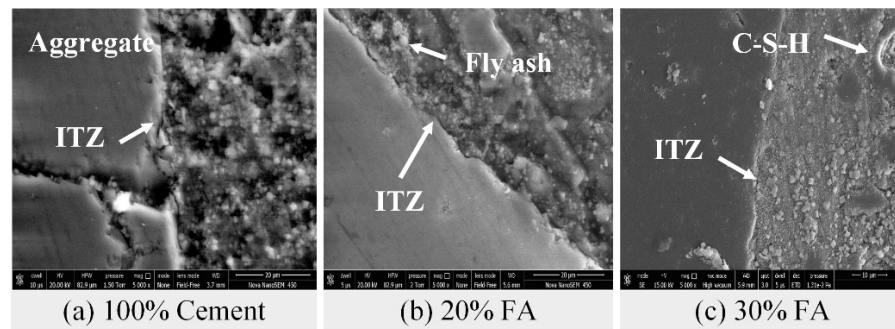


Figure 7. SEM images of SCC mixes at different levels of fly ash [25].

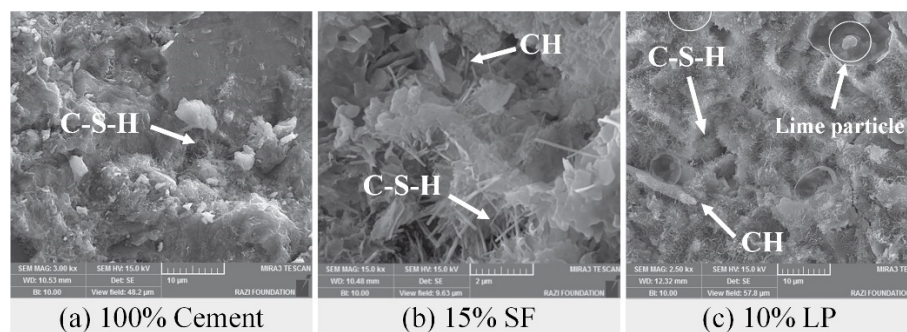


Figure 8. SEM images of SCC mixed with SF and LP [33].

4.2. Fresh Properties

Fluidity is the most common performance of fresh concrete, which engineers always primarily consider. On one hand, SCMs in SCC may fill the pores and lower the pore water content, increasing the quantity of free water and wrapping around the surface of the powder particles to produce a uniform water film that lubricates the paste and minimizes friction [77]. On the other hand, the increased specific surface area of some ground SCMs will improve water absorption and decrease free water content. Therefore, the fineness and proportion of SCMs have a significant impact on the fresh properties of SCC. Furthermore, because certain SCMs may reduce fluidity, superplasticizers are often necessary in SCC to improve the performance of the fresh mixture. The superplasticizer mainly disperses the powder particles via steric repulsion. When one end of the superplasticizer is adsorbed to the surface of the powder particles, the long chain at the other end generates physical barriers to prevent the surrounding cement particles from aggregation [78,79]. It is worth noting that the superplasticizers added to the SCC may have negative consequences. Existing studies have shown that the adsorption of these chemical admixtures on cement particles might retard the early hydration and result in a delayed setting [80].

A good deal of research has demonstrated that fly ash can increase the fluidity of the fresh SCC. This effect can be attributed to the smooth and spherical particles of FA [81]. Jain et al. [25] reported that the spherical particles of FA provided a ball-bearing action in newly mixed SCC, reducing the frictional resistance of aggregate particles. Promsawat et al. [23] reported similar findings. In addition, Sonebi [82] proposed that adding FA could enhance the fluidity by thickening the water film. However, FA may have negative effects on the fresh properties of SCC. Duran-Herrera et al. [22] found that FA prolongs the setting time of SCC.

Unlike fly ash, silica fume increases the water demand and decreases the fluidity due to its larger specific area. Choudhary et al. [17] observed the microscopic morphology of FA and SF (Figure 3) and discovered that spherical FA helps to reduce the friction between particles and improve fluidity. However, SF decreases fluidity and increases the superplasticizer demands due to its larger specific surface area and rough surface texture. As shown in Figure 9, Mustapha et al. [8] investigated the effects of FA and SF on the fresh

properties of SCC and discovered that FA improved the slump flow diameter (fluidity) but decreased the V-Funnel time (viscosity), whereas SF decreased the fluidity but increased the viscosity of SCC.

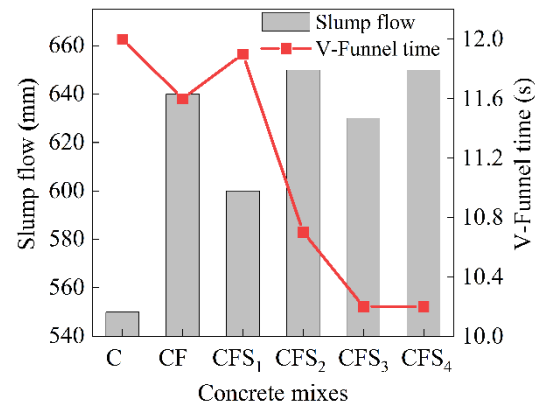


Figure 9. The slump flow and V-funnel time of SCC, adding FA and SF [8].

The impact of GBFS on the fresh properties of SCC is connected to the fineness and admixture proportion. Through the study of Boukendakdji [44], GBFS with a specific surface area of $350 \text{ m}^2/\text{kg}$ was utilized to substitute cement (Figure 10), with an ideal admixture rate of 15%. Furthermore, it was shown that GBFS has a superior water retention effect at increasing fineness, which minimizes the time-dependent loss of slump flow diameter. In contrast, Selvarani et al. [83] discovered that GBFS inclusion lowers the fluidity of SCC. Moreover, Ofuyatan et al. [84] reported that GBFS had a minimal influence on fresh properties, with an increase in incorporation from 10% to 30%, causing a 5% drop in slump flow diameter. This discrepancy can be attributed to two aspects: the differences in filling effect and specific surface area of varying fineness, and the changes in GBFS adsorption capability by various superplasticizers.

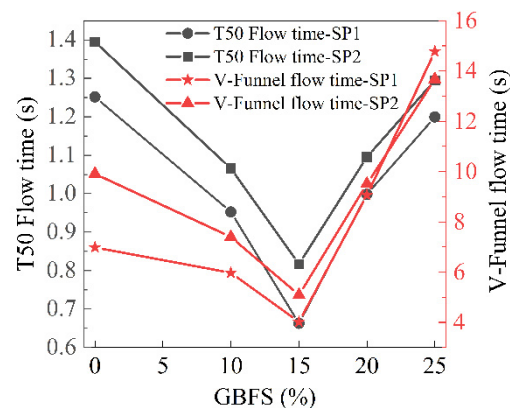


Figure 10. The effect of GBSF content on the T50 flow time and V-Funnel flow time of SCC (SP1 is a polycarboxylate-based superplasticizer and SP2 is a naphthalene sulphonate-based superplasticizer) [44].

The influence of LP on the fresh properties of SCC is mostly determined by its fineness. The filling effect of LP enhances the fluidity of the paste, but a higher content of finer powders increases the water requirement. Sua-iam et al. [56,57] found that mixing LP with a median particle size of $15.63 \mu\text{m}$ ($D_{50 \text{ cement}} = 23.30 \mu\text{m}$) increased water demand and reduced fluidity. Faheem [61] discovered that mixing LP with a median particle size of $11.60 \mu\text{m}$ ($D_{50 \text{ cement}} = 15.32 \mu\text{m}$) also reduced fluidity. Celik et al. [58,59] showed that LP with an average particle size of $48.1 \mu\text{m}$ ($D_{\text{cement}} = 10.4 \mu\text{m}$) enhances fluidity and shortens setting time, and that about 15% of the LP in the experiment enhanced slump flow diameter

by 7%. In addition, some research revealed that there is a discrepancy in the compatibility of LP with various superplasticizers [62].

4.3. Strength Properties

The effect of SCMs on the strength properties of SCC is influenced by the filler effect, the pozzolanic reaction, and the dilution effect. The partial substitution of cement by SCMs reduces the cementitious component of the paste, hence slowing the development of early strength. FA is predominantly composed of SiO_2 and Al_2O_3 with minimal pozzolanic reactivity, and it typically facilitates post-strength growth [81]. Mahalingam et al. [21] reported that using 40% FA replacement of cement has a considerable diluting effect and lowers compressive strength. Esquinas et al. [15] also found that using FA delayed the strength development of SCC. According to the research of Altoubat et al. [85], incorporating 50% FA into SCC not only had a negative influence on early strength but also increased shrinkage. The ideal quantity of FA should not exceed 35%; otherwise, silica fume should be added to encourage the development of strength (Figure 11).

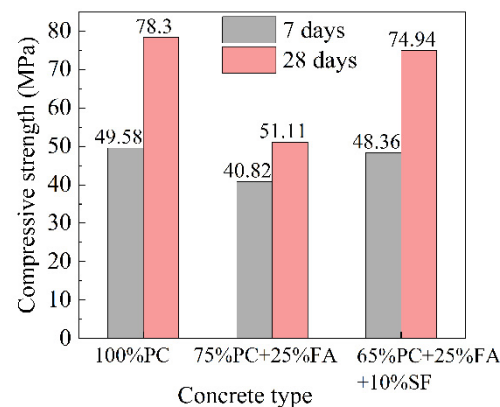


Figure 11. Effect of FA and SF on the compressive strength of SCC [8].

In contrast, SF with high fineness and pozzolanic reactivity frequently enhances the strength properties of SCC [9]. From the results of Fakhri [86,87], the incorporation of 10% SF can improve the compressive strength by more than 30% and increase the flexural strength by around 20%; the addition of 25% SF can optimize the flexural strength by approximately 40%. According to Karthik et al. [88], this is because SF contains a high content of reactive SiO_2 , which might enhance the hydration. Furthermore, SF may efficiently enhance the filler effect and improve the interfacial transition zone. Esfandiari et al. [33] indicated that the reactive SiO_2 in SF could effectively react with $\text{Ca}(\text{OH})_2$ in the paste to generate C-S-H gels.

The substitution of GBFS for cement in SCC will delay the early strength growth of the paste [8]. Boukendakdji et al. [44] researched the influence of GBFS on SCC and discovered that the early compressive strength of concrete reduced as GBFS admixture increased, but the post-strength (at 56 days and 90 days) did not appreciably decrease (Figure 12). Altoubat et al. [89] also discovered that GBFS lowers the strength of SCC, with the 28-day compressive strength decreasing by around 10% at 70% admixture, while Ofuyatan et al. [84] discovered that GBFS has a negligible influence on the strength development of SCC, with 28-day compressive strength rising by just 1% at 20% substitution and dropping by 4% at 30% substitution. Furthermore, Dadsetan et al. [47] revealed that the effect of GBFS on the strength of SCC is related to the water–cement ratio and the content of GBFS. The experimental results showed that at a water–cement ratio of 0.4, the 7-day and the 28-day compressive strengths of concrete with 10%, 20%, and 30% GBFS admixture were all reduced. However, at a water–cement ratio of 0.45, the 7-day and 28-day compressive strengths of concrete with all three admixtures increased. With the 30% admixture, the 28-day strength increased by about 30%.

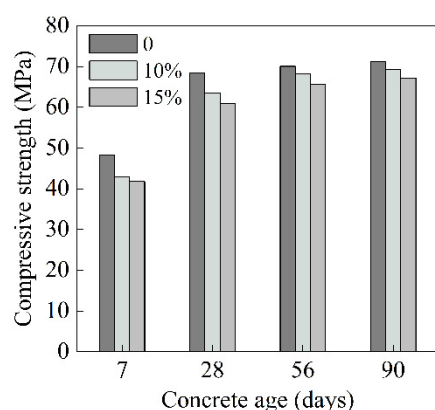


Figure 12. Variations of compressive strength with GBFS content of concrete [44].

LP stimulates the hydration of cement and enhances the strength development of concrete primarily through the adsorption of Ca^{2+} by CaCO_3 , which promotes the dissolution of C_3S . At the beginning of the cement hydration, the dissolution and hydration of C_3S produce a substantial quantity of Ca^{2+} . Since Ca^{2+} has a stronger migration capacity than SiO_3^{2-} , the chemical adsorption of CaCO_3 to Ca^{2+} happens when Ca^{2+} diffuses toward the surface of LP particles. On one hand, this adsorption decreases the concentration of Ca^{2+} around the C_3S particles, allowing C_3S to dissolve and hydrate more quickly. On the other hand, the connection of Ca^{2+} with the surface of LP particles causes them to form ion clusters, which continue to expand to construct the crystal nucleus and gradually grow into C-S-H gels. Therefore, the adsorption of Ca^{2+} by the surface of LP greatly promotes the hydration of cement and leads to the high-density nucleation and directional growth of C-S-H [75].

4.4. Durability Properties

The compactness of the paste greatly influences the durability of concrete [90,91]. The diluting effect of SCMs decreases the quantity of cement, lowering the temperature increase in concrete and minimizing the risks of cracking [82]. Altoubat et al. [89] demonstrated that incorporating GBFS and FA decreased the internal stress of SCC, resulting in better cracking resistance (Figure 13). The filling effect of SCMs may reduce the porosity and permeability by packing the pores of the paste, thus improving the durability of SCC. For example, SF may increase the durability of SCC by filling the pores to reinforce the microstructure. According to the research of Karthik et al. [88], SCC exhibited higher resistance to sulfate attack and chloride ion penetration with the addition of SF admixture. Esfandiari et al. [33] suggested that this is not only due to the filling effect of SF but also the pozzolanic reaction, which is SF reacting with CH to produce C-S-H. Additionally, Sideris et al. [49] reported that the filling effect with the addition of GBFS in SCC decreased the porosity and reduced the carbonation depth. Zhang [92] proposed that GBFS could effectively improve the sulfate attack resistance of concrete. Moreover, Zhu et al. [62] claimed that the smaller the particle size of the LP, the better it filled the pores and the greater the packing density. The adsorption effect of LP on cement hydration is beneficial for enhancing the microstructure.

It should be noted that FA has a significant impact on the resistance to chloride ion penetration of SCC. Gnanaraj et al. [93] discovered that FA could greatly enhance its resistance to chloride ion penetration. The studies of Mahalingam et al. [21] and Esquinas et al. [14,15] also came up with similar outcomes. Dinakar et al. [24] indicated that the resistance to both sulfate attack and chloride ion penetration is noticeably increased with the increasing FA content. This is because the permeability of chloride ions relies on the chloride binding capacity of the substance. The Cl^- penetrates into the interior concrete along with the water, and some of the chlorides can react with the mineral phase in cement (mainly aluminum-containing) to form stable chlorine-containing complexes. However, when the chloride is supersaturated, a certain amount of the free state Cl^- is produced, which will corrode the

concrete. It is widely known that FA contains a high proportion of aluminum-containing mineral phases. Figure 2 also illustrates that the concentration of Al_2O_3 in FA is greater than that in cement. Therefore, as the FA proportion rises, the chloride-binding capacity of SCC also increases, limiting the concentration of free Cl^- that might cause corrosion. Similarly, GBFS contains more aluminum phase minerals than cement, and Sideris et al. [49] reported that GBFS can increase the resistance to chloride ion penetration of SCC.

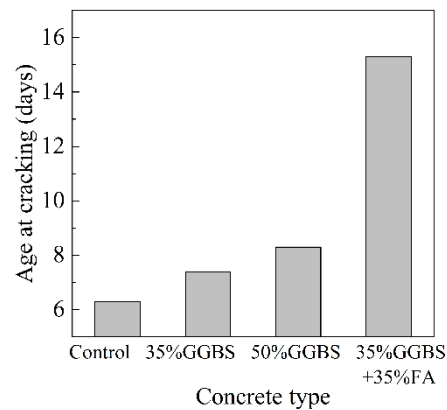


Figure 13. Ages at cracking of SCC, adding GBFS and FA [87].

5. Conclusions

The application techniques and hydration mechanisms of SCMs in SCC were discussed, and the impacts of FA, SF, GBFS, and LP on the microstructure and performance of SCC were reviewed. The major conclusions are as follows:

- SCC has a high content of powder material, and it is feasible to reduce the quantity of cement and thus decrease the production costs by incorporating SCMs. FA, SF, GBFS, and LP are the most frequently utilized SCMs in SCC. FA contains a high proportion of aluminum phase and predominantly spherical particles; SF primarily contains SiO_2 and has a high specific surface area. GBFS mainly contains SiO_2 and CaO ; LP chiefly consists of CaCO_3 , and both of them show obvious irregular and angular shapes due to mechanical grinding. The hydration mechanisms of these SCMs in SCC include pozzolanic reaction, alkaline activation, and adsorption effect. Moreover, the filling effect and dilution effect of some SCMs on the paste will contribute to reducing the porosity and limiting the temperature rise of concrete, respectively.
- The spherical particles of FA improve the fluidity of the freshly mixed paste, whereas SF increases the water demand and reduces fluidity due to its large specific surface area. The effect of GBFS on the fresh properties of SCC is related to the fineness and blending amount. The impact of LP is determined by the fineness, and LP will typically increase water consumption. Furthermore, superplasticizers are often added into SCC to increase the fresh properties, and superplasticizers might retard the early hydration and result in a delayed setting.
- The low pozzolanic reactivity of FA typically decreases the strength properties, particularly the early strength; the active SF usually enhances strength. The effect of GBFS on strength is dependent on the water–cement ratio and admixture amount, and it usually reduces the early strength while having little effect on post-strength. The adsorption effect of CaCO_3 on Ca^{2+} in LP will accelerate the hydration of cement and improve the development of the early strength.
- The pozzolanic reaction and filling effect of SCMs reduce the porosity of the hardened paste, resulting in a denser microstructure in the interfacial transition zone, thus increasing the durability of SCC. Furthermore, because of the high aluminum phase composition, FA and GBFS are typically capable of improving the resistance to chloride ion penetration and sulfate attack of SCC.

It is worth mentioning that although the employment of multiple SCMs in a composite system may provide a superposition effect, the chemical composition of different SCMs varies widely, and the issues of compatibility may rise. The rules governing the influence of composite SCMs added to SCC are not consistent and require additional investigation.

Author Contributions: Conceptualization, Z.L. and D.W.; validation, Z.L., M.A. and D.W.; investigation, L.P.; resources, Z.L.; writing—original draft preparation, L.P.; writing—review and editing, D.W.; visualization, L.P.; supervision, D.W.; project administration, D.W. All authors have read and agreed to the published version of the manuscript.

Funding: This work was funded by Natural Science Foundation of China [No. 51478248].

Acknowledgments: The authors would like to acknowledge the National Natural Science Foundation of China (No. 51478248).

Conflicts of Interest: The authors declare that they have no known competing financial interests or personal relationships that could have appeared to influence the work reported in this paper.

References

1. Okamura, H.; Ouchi, M. Self-compacting concrete. *J. Adv. Concr. Technol.* **2003**, *1*, 5–15. [CrossRef]
2. Global Cement Production Top Countries 2020 | Statista. Available online: <https://www.statista.com/statistics/267364/world-cement-production-by-country/> (accessed on 1 December 2021).
3. Wang, D.; Wang, Q.; Xue, J. Reuse of hazardous electrolytic manganese residue: Detailed leaching characterization and novel application as a cementitious material. *Resour. Conserv. Recy.* **2020**, *154*, 104645. [CrossRef]
4. Xie, T.; Mohamad Ali, M.S.; Elchalakani, M.; Visintin, P. Modelling fresh and hardened properties of self-compacting concrete containing supplementary cementitious materials using reactive moduli. *Constr. Build. Mater.* **2021**, *272*, 121954. [CrossRef]
5. Wu, Q.; An, X. Development of a mix design method for SCC based on the rheological characteristics of paste. *Constr. Build. Mater.* **2014**, *53*, 642–651. [CrossRef]
6. Nie, D.; An, X. Optimization of SCC mix at paste level by using numerical method based on a paste rheological threshold theory. *Constr. Build. Mater.* **2016**, *102*, 428–434. [CrossRef]
7. Domone, P.L. Self-compacting concrete: An analysis of 11 years of case studies. *Cem. Con. Comp.* **2006**, *28*, 197–208. [CrossRef]
8. Mustapha, F.A.; Sulaiman, A.; Mohamed, R.N.; Umara, S.A. The effect of fly ash and silica fume on self-compacting high-performance concrete. *Mater. Tod. Proceed.* **2021**, *39*, 965–969. [CrossRef]
9. Benaicha, M.; Roguiez, X.; Jalbaud, O.; Burtschell, Y.; Alaoui, A.H. Influence of silica fume and viscosity modifying agent on the mechanical and rheological behavior of self compacting concrete. *Constr. Build. Mater.* **2015**, *84*, 103–110. [CrossRef]
10. Lachemi, M.; Hossain, K.M.A.; Lambros, V.; Nkinamubanzi, P.C.; Bouzoubaâ, N. Self-consolidating concrete incorporating new viscosity modifying admixtures. *Cem. Con. Res.* **2004**, *34*, 917–926. [CrossRef]
11. Gupta, N.; Siddique, R.; Belarbi, R. Sustainable and Greener Self-Compacting Concrete incorporating Industrial By-Products: A Review. *J. Clean. Prod.* **2021**, *284*, 124803. [CrossRef]
12. Sai Teja, G.; Ravella, D.P.; Chandra Sekhara Rao, P.V. Studies on self-curing self-compacting concretes containing zeolite admixture. *Mater. Tod. Proceed.* **2021**, *43*, 2355–2360. [CrossRef]
13. Ponikiewski, T.; Gołaszewski, J. The influence of high-calcium fly ash on the properties of fresh and hardened self-compacting concrete and high performance self-compacting concrete. *J. Clean. Prod.* **2014**, *72*, 212–221. [CrossRef]
14. Esquinas, A.R.; Álvarez, J.I.; Jiménez, J.R.; Fernández, J.M. Durability of self-compacting concrete made from non-conforming fly ash from coal-fired power plants. *Constr. Build. Mater.* **2018**, *189*, 993–1006. [CrossRef]
15. Esquinas, A.R.; Ledesma, E.F.; Otero, R.; Jiménez, J.R.; Fernández, J.M. Mechanical behaviour of self-compacting concrete made with non-conforming fly ash from coal-fired power plants. *Constr. Build. Mater.* **2018**, *182*, 385–398. [CrossRef]
16. Singh, N.; Kumar, P.; Goyal, P. Reviewing the behaviour of high volume fly ash based self compacting concrete. *J. Build. Eng.* **2019**, *26*, 100882. [CrossRef]
17. Choudhary, R.; Gupta, R.; Nagar, R. Impact on fresh, mechanical, and microstructural properties of high strength self-compacting concrete by marble cutting slurry waste, fly ash, and silica fume. *Constr. Build. Mater.* **2020**, *239*, 117888. [CrossRef]
18. Choudhary, R.; Gupta, R.; Alomayri, T.; Jain, A.; Nagar, R. Permeation, corrosion, and drying shrinkage assessment of self-compacting high strength concrete comprising waste marble slurry and fly ash, with silica fume. *Structures* **2021**, *33*, 971–985. [CrossRef]
19. Mohammed, A.M.; Asaad, D.S.; Al-Hadithi, A.I. Experimental and statistical evaluation of rheological properties of self-compacting concrete containing fly ash and ground granulated blast furnace slag. *J. King Saud Univ. Eng. Sci.* **2021**. [CrossRef]
20. Prakash, R.; Raman, S.N.; Divyah, N.; Subramanian, C.; Vijayaprabha, C.; Praveenkumar, S. Fresh and mechanical characteristics of roselle fibre reinforced self-compacting concrete incorporating fly ash and metakaolin. *Constr. Build. Mater.* **2021**, *290*, 123209. [CrossRef]

21. Mahalingam, B.; Nagamani, K.; Kannan, L.S.; Mohammed Haneefa, K.; Bahurudeen, A. Assessment of hardened characteristics of raw fly ash blended self-compacting concrete. *Persp. Sci.* **2016**, *8*, 709–711. [[CrossRef](#)]
22. Duran-Herrera, A.; De-León-Esquivel, J.; Bentz, D.P.; Valdez-Tamez, P. Self-compacting concretes using fly ash and fine limestone powder: Shrinkage and surface electrical resistivity of equivalent mortars. *Constr. Build. Mater.* **2019**, *199*, 50–62. [[CrossRef](#)]
23. Promsawat, P.; Chatveera, B.; Sua-iam, G.; Makul, N. Properties of self-compacting concrete prepared with ternary Portland cement-high volume fly ash-calcium carbonate blends. *Case Stud. Constr. Mat.* **2020**, *13*, e00426. [[CrossRef](#)]
24. Dinakar, P.; Babu, K.G.; Santhanam, M. Durability properties of high volume fly ash self compacting concretes. *Cem. Con. Comp.* **2008**, *30*, 880–886. [[CrossRef](#)]
25. Jain, A.; Gupta, R.; Chaudhary, S. Sustainable development of self-compacting concrete by using granite waste and fly ash. *Constr. Build. Mater.* **2020**, *262*, 120516. [[CrossRef](#)]
26. Akcay, B.; Tasdemir, M.A. Performance evaluation of silica fume and metakaolin with identical finenesses in self compacting and fiber reinforced concretes. *Constr. Build. Mater.* **2018**, *185*, 436–444. [[CrossRef](#)]
27. Bani Ardalan, R.; Joshaghani, A.; Hooton, R.D. Workability retention and compressive strength of self-compacting concrete incorporating pumice powder and silica fume. *Constr. Build. Mater.* **2017**, *134*, 116–122. [[CrossRef](#)]
28. Wongkeo, W.; Thongsanitgarn, P.; Ngamjarujana, A.; Chaipanich, A. Compressive strength and chloride resistance of self-compacting concrete containing high level fly ash and silica fume. *Mater. Design.* **2014**, *64*, 261–269. [[CrossRef](#)]
29. Mastali, M.; Dalvand, A. Use of silica fume and recycled steel fibers in self-compacting concrete (SCC). *Constr. Build. Mater.* **2016**, *125*, 196–209. [[CrossRef](#)]
30. Ghoddousi, P.; Adelzade Saadabadi, L. Study on hydration products by electrical resistivity for self-compacting concrete with silica fume and metakaolin. *Constr. Build. Mater.* **2017**, *154*, 219–228. [[CrossRef](#)]
31. Bernal, J.; Reyes, E.; Massana, J.; León, N.; Sánchez, E. Fresh and mechanical behavior of a self-compacting concrete with additions of nano-silica, silica fume and ternary mixtures. *Constr. Build. Mater.* **2018**, *160*, 196–210. [[CrossRef](#)]
32. Zarnaghi, V.N.; Fouroghi-Asl, A.; Nourani, V.; Ma, H. On the pore structures of lightweight self-compacting concrete containing silica fume. *Constr. Build. Mater.* **2018**, *193*, 557–564. [[CrossRef](#)]
33. Esfandiari, J.; Loghmani, P. Effect of perlite powder and silica fume on the compressive strength and microstructural characterization of self-compacting concrete with lime-cement binder. *Measurement* **2019**, *147*, 106846. [[CrossRef](#)]
34. Salehi, H.; Mazloom, M. Opposite effects of ground granulated blast-furnace slag and silica fume on the fracture behavior of self-compacting lightweight concrete. *Constr. Build. Mater.* **2019**, *222*, 622–632. [[CrossRef](#)]
35. Sasanipour, H.; Aslani, F. Effect of specimen shape, silica fume, and curing age on durability properties of self-compacting concrete incorporating coarse recycled concrete aggregates. *Constr. Build. Mater.* **2019**, *228*, 117054. [[CrossRef](#)]
36. Sasanipour, H.; Aslani, F.; Taherinezhad, J. Effect of silica fume on durability of self-compacting concrete made with waste recycled concrete aggregates. *Constr. Build. Mater.* **2019**, *227*, 116598. [[CrossRef](#)]
37. Guo, Z.; Jiang, T.; Zhang, J.; Kong, X.; Chen, C.; Lehman, D.E. Mechanical and durability properties of sustainable self-compacting concrete with recycled concrete aggregate and fly ash, slag and silica fume. *Constr. Build. Mater.* **2020**, *231*, 117115. [[CrossRef](#)]
38. Mahalakshmi, S.H.V.; Khed, V.C. Experimental study on M-sand in self-compacting concrete with and without silica fume. *Mater. Tod. Proceed.* **2020**, *27*, 1061–1065. [[CrossRef](#)]
39. Faraj, R.H.; Sherwani, A.F.H.; Jafer, L.H.; Ibrahim, D.F. Rheological behavior and fresh properties of self-compacting high strength concrete containing recycled PP particles with fly ash and silica fume blended. *J. Build. Eng.* **2021**, *34*, 101667. [[CrossRef](#)]
40. Saba, A.M.; Khan, A.H.; Akhtar, M.N.; Khan, N.A.; Rahimian Kolor, S.S.; Petru, M.; Radwan, N. Strength and flexural behavior of steel fiber and silica fume incorporated self-compacting concrete. *J. Mater. Res. Technol.* **2021**, *12*, 1380–1390. [[CrossRef](#)]
41. Manikanta, D.; Ravella, D.P. Mechanical and durability characteristics of high performance self-compacting concrete containing flyash, silica fume and graphene oxide. *Mater. Tod. Proceed.* **2021**, *43*, 2361–2367. [[CrossRef](#)]
42. Vejmelková, E.; Keppert, M.; Grzeszczyk, S.; Skaliński, B.; Černý, R. Properties of self-compacting concrete mixtures containing metakaolin and blast furnace slag. *Constr. Build. Mater.* **2011**, *25*, 1325–1331. [[CrossRef](#)]
43. Ting, L.; Qiang, W.; Shiyu, Z. Effects of ultra-fine ground granulated blast-furnace slag on initial setting time, fluidity and rheological properties of cement pastes. *Powder Technol.* **2019**, *345*, 54–63. [[CrossRef](#)]
44. Boukendakdji, O.; Kadri, E.-H.; Kenai, S. Effects of granulated blast furnace slag and superplasticizer type on the fresh properties and compressive strength of self-compacting concrete. *Cem. Con. Comp.* **2012**, *34*, 583–590. [[CrossRef](#)]
45. Anastasiou, E.K.; Papayianni, I.; Papachristoforou, M. Behavior of self compacting concrete containing ladle furnace slag and steel fiber reinforcement. *Mater. Design.* **2014**, *59*, 454–460. [[CrossRef](#)]
46. Valcuende, M.; Benito, F.; Parra, C.; Miñano, I. Shrinkage of self-compacting concrete made with blast furnace slag as fine aggregate. *Constr. Build. Mater.* **2015**, *76*, 1–9. [[CrossRef](#)]
47. Dadsetan, S.; Bai, J. Mechanical and microstructural properties of self-compacting concrete blended with metakaolin, ground granulated blast-furnace slag and fly ash. *Constr. Build. Mater.* **2017**, *146*, 658–667. [[CrossRef](#)]
48. Patel, Y.J.; Shah, N. Enhancement of the properties of Ground Granulated Blast Furnace Slag based Self Compacting Geopolymer Concrete by incorporating Rice Husk Ash. *Constr. Build. Mater.* **2018**, *171*, 654–662. [[CrossRef](#)]
49. Sideris, K.K.; Tassos, C.; Chatzopoulos, A.; Manita, P. Mechanical characteristics and durability of self compacting concretes produced with ladle furnace slag. *Constr. Build. Mater.* **2018**, *170*, 660–667. [[CrossRef](#)]

50. de Matos, P.R.; Oliveira, J.C.P.; Medina, T.M.; Magalhães, D.C.; Gleize, P.J.P.; Schankoski, R.A.; Pilar, R. Use of air-cooled blast furnace slag as supplementary cementitious material for self-compacting concrete production. *Constr. Build. Mater.* **2020**, *262*, 120102. [[CrossRef](#)]
51. Santamaría, A.; Ortega-López, V.; Skaf, M.; Chica, J.A.; Manso, J.M. The study of properties and behavior of self compacting concrete containing Electric Arc Furnace Slag (EAFS) as aggregate. *Ain Shams Eng. J.* **2020**, *11*, 231–243. [[CrossRef](#)]
52. Boukendakdji, O.; Kenai, S.; Kadri, E.H.; Rouis, F. Effect of slag on the rheology of fresh self-compacted concrete. *Constr. Build. Mater.* **2009**, *23*, 2593–2598. [[CrossRef](#)]
53. Zhao, H.; Sun, W.; Wu, X.; Gao, B. The properties of the self-compacting concrete with fly ash and ground granulated blast furnace slag mineral admixtures. *J. Clean. Prod.* **2015**, *95*, 66–74. [[CrossRef](#)]
54. Wang, D.; Wang, Q.; Huang, Z. New insights into the early reaction of NaOH-activated slag in the presence of CaSO₄. *Compos. Part B-Eng.* **2020**, *198*, 108207. [[CrossRef](#)]
55. Rizwan, S.A.; Bier, T.A. Blends of limestone powder and fly-ash enhance the response of self-compacting mortars. *Constr. Build. Mater.* **2012**, *27*, 398–403. [[CrossRef](#)]
56. Sua-iam, G.; Makul, N. Utilization of limestone powder to improve the properties of self-compacting concrete incorporating high volumes of untreated rice husk ash as fine aggregate. *Constr. Build. Mater.* **2013**, *38*, 455–464. [[CrossRef](#)]
57. Sua-iam, G.; Makul, N. Use of increasing amounts of bagasse ash waste to produce self-compacting concrete by adding limestone powder waste. *J. Clean. Prod.* **2013**, *57*, 308–319. [[CrossRef](#)]
58. Celik, K.; Jackson, M.D.; Mancio, M.; Meral, C.; Emwas, A.H.; Mehta, P.K.; Monteiro, P.J.M. High-volume natural volcanic pozzolan and limestone powder as partial replacements for portland cement in self-compacting and sustainable concrete. *Cem. Con. Comp.* **2014**, *45*, 136–147. [[CrossRef](#)]
59. Celik, K.; Meral, C.; Petek Gursel, A.; Mehta, P.K.; Horvath, A.; Monteiro, P.J.M. Mechanical properties, durability, and life-cycle assessment of self-consolidating concrete mixtures made with blended portland cements containing fly ash and limestone powder. *Cem. Con. Comp.* **2015**, *56*, 59–72. [[CrossRef](#)]
60. Benjeddou, O.; Soussi, C.; Jedidi, M.; Benali, M. Experimental and theoretical study of the effect of the particle size of limestone fillers on the rheology of self-compacting concrete. *J. Build. Eng.* **2017**, *10*, 32–41. [[CrossRef](#)]
61. Faheem, A.; Rizwan, S.A.; Bier, T.A. Properties of self-compacting mortars using blends of limestone powder, fly ash, and zeolite powder. *Constr. Build. Mater.* **2021**, *286*, 122788. [[CrossRef](#)]
62. Zhu, W.; Bartos, P. Microstructure and Properties of Interfacial Transition Zone in SCC. In Proceedings of the First International Symposium on Design Performance and use of Self Consolidating Concrete, RILEM Publications SARL, Changsha, China, 26–28 May 2005; pp. 319–327.
63. Gesoğlu, M.; Güneş, E.; Kocabağ, M.E.; Bayram, V.; Mermerdaş, K. Fresh and hardened characteristics of self compacting concretes made with combined use of marble powder, limestone filler, and fly ash. *Constr. Build. Mater.* **2012**, *37*, 160–170. [[CrossRef](#)]
64. Zhuang, S.; Wang, Q. Inhibition mechanisms of steel slag on the early-age hydration of cement. *Cem. Con. Res.* **2021**, *140*, 106283. [[CrossRef](#)]
65. Yang, S.; Zhang, J.; An, X.; Qi, B.; Shen, D.; Lv, M. Effects of fly ash and limestone powder on the paste rheological thresholds of self-compacting concrete. *Constr. Build. Mater.* **2021**, *281*, 122560. [[CrossRef](#)]
66. Chinthakunta, R.; Ravella, D.P.; Sri Rama Chand, M.; Janardhan Yadav, M. Performance evaluation of self-compacting concrete containing fly ash, silica fume and nano titanium oxide. *Mater. Tod. Proceed.* **2021**, *43*, 2348–2354. [[CrossRef](#)]
67. Zhu, W.; Gibbs, J.C. Use of different limestone and chalk powders in self-compacting concrete. *Cem. Con. Res.* **2005**, *35*, 1457–1462. [[CrossRef](#)]
68. Scrivener, K.; Ouzia, A.; Juilland, P.; Kunhi Mohamed, A. Advances in understanding cement hydration mechanisms. *Cem. Con. Res.* **2019**, *124*, 105823. [[CrossRef](#)]
69. Provis, J.L.; Van Deventer, J.S. *Alkali Activated Materials: State-of-the-Art Report*; RILEM TC 224-AAM; Springer: Dordrecht, The Netherlands, 2014; Volume 13, ISBN 978-94-007-7671-5.
70. Provis, J.L.; Palomo, A.; Shi, C. Advances in understanding alkali-activated materials. *Cem. Con. Res.* **2015**, *78*, 110–125. [[CrossRef](#)]
71. Ben Haha, M.; Le Saout, G.; Winnefeld, F.; Lothenbach, B. Influence of activator type on hydration kinetics, hydrate assemblage and microstructural development of alkali activated blast-furnace slags. *Cem. Con. Res.* **2011**, *41*, 301–310. [[CrossRef](#)]
72. Myers, R.J.; Bernal, S.A.; San Nicolas, R.; Provis, J.L. Generalized structural description of calcium-sodium aluminosilicate hydrate gels: The cross-linked substituted tobermorite model. *Langmuir* **2013**, *29*, 5294–5306. [[CrossRef](#)]
73. Yalçınkaya, Ç.; Çopuroğlu, O. Hydration heat, strength and microstructure characteristics of UHPC containing blast furnace slag. *J. Build. Eng.* **2021**, *34*, 101915. [[CrossRef](#)]
74. Fernández-Jiménez, A.; Palomo, A.; Criado, M. Microstructure development of alkali-activated fly ash cement: A descriptive model. *Cem. Con. Res.* **2005**, *35*, 1204–1209. [[CrossRef](#)]
75. Ouyang, X.; Xu, S.; Ma, Y.; Ye, G. Effect of Aggregate Chemical Properties on Nucleation and Growth of Calcium Silicate Hydrate C-S-H. Kuei Suan Jen Hsueh Pao. *J. Chin. Ceram. Soc.* **2021**, *49*, 972–979. [[CrossRef](#)]
76. Mehta, P.K.; Monteiro, P.J. *Concrete: Microstructure, Properties, and Materials*; McGraw-Hill Education: New York, NY, USA, 2014.
77. Li, L.G.; Kwan, A.K.H. Concrete mix design based on water film thickness and paste film thickness. *Cem. Con. Comp.* **2013**, *39*, 33–42. [[CrossRef](#)]

78. Zhang, Y.; Kong, X. Correlations of the dispersing capability of NSF and PCE types of superplasticizer and their impacts on cement hydration with the adsorption in fresh cement pastes. *Cem. Con. Res.* **2015**, *69*, 1–9. [[CrossRef](#)]
79. Wang, D.; Wang, Q.; Huang, Z. Investigation on the poor fluidity of electrically conductive cement-graphite paste: Experiment and simulation. *Mater. Design.* **2019**, *169*, 107679. [[CrossRef](#)]
80. Sha, S.; Wang, M.; Shi, C.; Xiao, Y. Influence of the structures of polycarboxylate superplasticizer on its performance in cement-based materials-A review. *Constr. Build. Mater.* **2020**, *233*, 117257. [[CrossRef](#)]
81. Alexandra, C.; Bogdan, H.; Camelia, N.; Zoltan, K. Mix design of self-compacting concrete with limestone filler versus fly ash addition. *Proced. Manufact.* **2018**, *22*, 301–308. [[CrossRef](#)]
82. Sonebi, M. Medium strength self-compacting concrete containing fly ash: Modelling using factorial experimental plans. *Cem. Con. Res.* **2004**, *34*, 1199–1208. [[CrossRef](#)]
83. Selvarani, B.; Preethi, V. Investigational study on optimum content of GGBS and fibres in fibre non-breakable self compacting concrete. *Mater. Tod. Proceed.* **2021**, *47*, 6111–6115. [[CrossRef](#)]
84. Ofuyatan, O.M.; Adeniyi, A.G.; Ijje, D.; Ighalo, J.O.; Oluwafemi, J. Development of high-performance self compacting concrete using eggshell powder and blast furnace slag as partial cement replacement. *Constr. Build. Mater.* **2020**, *256*, 119403. [[CrossRef](#)]
85. Altoubat, S.; Talha Junaid, M.; Leblouba, M.; Badran, D. Effectiveness of fly ash on the restrained shrinkage cracking resistance of self-compacting concrete. *Cem. Con. Comp.* **2017**, *79*, 9–20. [[CrossRef](#)]
86. Fakhri, M.; Yousefian, F.; Amosoltani, E.; Aliha, M.R.M.; Berto, F. Combined Effects of Recycled Crumb Rubber and Silica Fume on Mechanical Properties and Mode I Fracture Toughness of Self-compacting Concrete. *Fatigue Fract. Eng. Mater. Struct.* **2021**, *44*, 2659–2673. [[CrossRef](#)]
87. Fakhri, M.; Saberi., K.F. The Effect of Waste Rubber Particles and Silica Fume on the Mechanical Properties of Roller Compacted Concrete Pavement. *J. Clean. Prod.* **2016**, *129*, 521–530. [[CrossRef](#)]
88. Karthik, D.; Nirmalkumar, K.; Priyadharshini, R. Characteristic assessment of self-compacting concrete with supplementary cementitious materials. *Constr. Build. Mater.* **2021**, *297*, 123845. [[CrossRef](#)]
89. Altoubat, S.; Badran, D.; Junaid, M.T.; Leblouba, M. Restraint shrinkage behavior of Self-Compacting Concrete containing ground-granulated blast-furnace slag. *Constr. Build. Mater.* **2016**, *129*, 98–105. [[CrossRef](#)]
90. Bossio, A.; Lignola, G.P.; Fabbrocino, F.; Monetta, T.; Prota, A.; Bellucci, F.; Manfredi, G. Nondestructive Assessment of Corrosion of Reinforcing Bars through Surface Concrete Cracks. *Struct. Concr.* **2017**, *18*, 104–117. [[CrossRef](#)]
91. Pittella, E.; Angrisani, L.; Cataldo, A.; Piuze, E.; Fabbrocino, F. Embedded Split Ring Resonator Network for Health Monitoring in Concrete Structures. *IEEE Instrum. Meas. Mag.* **2020**, *23*, 14–20. [[CrossRef](#)]
92. Zhang, Z.; Wang, Q.; Chen, H.; Zhou, Y. Influence of the initial moist curing time on the sulfate attack resistance of concretes with different binders. *Constr. Build. Mater.* **2017**, *144*, 541–551. [[CrossRef](#)]
93. Gnanaraj, S.C.; Chokkalingam, R.B.; Thankam, G.L.; Pothinathan, S.K.M. Durability properties of self-compacting concrete developed with fly ash and ultra fine natural steatite powder. *J. Mater. Res. Technol.* **2021**, *13*, 431–439. [[CrossRef](#)]